Comparison of Silicon-Based Detectors

22nd Workshop for Radiation Monitoring on ISS

2017-09-06

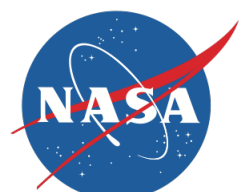

R. Rios, Ph.D.

Space Radiation
Analysis Group **NASA**

Introduction

Purpose

- Well-established history and pedigree of Silicon-based detectors on ISS, e.g., ALTEA, DB-8, DOSTEL, ISS-RAD, & REM.
- In this talk, we will take a quick look at data from co-located instruments:
  - DOSTEL and REM: spanning multiple years in Columbus.
    - Focusing on environment categorized dosimetry and energy loss.
  - RAD and REM: during the first ∼10 months of RAD's deployment in Destiny.
    - Focusing on environment categorized dosimetry.

Environment Definitions

There are many ways of categorizing GCR and the trapped/SAA environments; these definitions describe the scale and shape of the particle flux in each environment and affect spectral shapes.

Generalizing, LEO environment definitions fall into two categories:

1. Instrument-specific:
   - Typically provides a “purer” SAA measurement; shielding-modulated SAA environment is usually added into GCR.
     - Dose rate thresholds; count-rate thresholds.
2. Model-based:
   - Selection is arbitrary, but is typically used to provide a “purer” GCR measurement; transition from GCR to SAA is either added into the SAA or kept as separate.
     - Magnetic field intensity & L-shell; trapped proton model contributions at a location.

In the following comparisons, we will use multiple definitions.

Daily Dosimetry

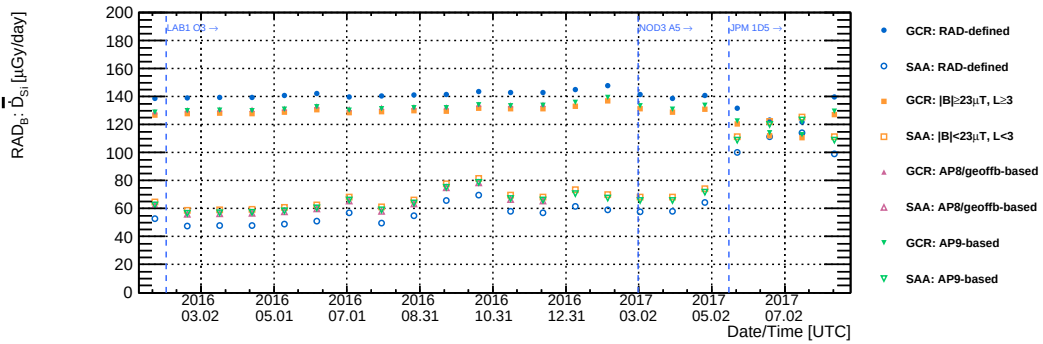

Figure 1: Average daily GCR/SAA dose rates in silicon per Bartel Rotation in RAD_B. Detector locations are indicated by annotated vertical lines. Only days for which there is more than 95% live time for [2016-02-01, 2017-08-07) are used in the calculations.

DOSTEL & REM

Detector Location

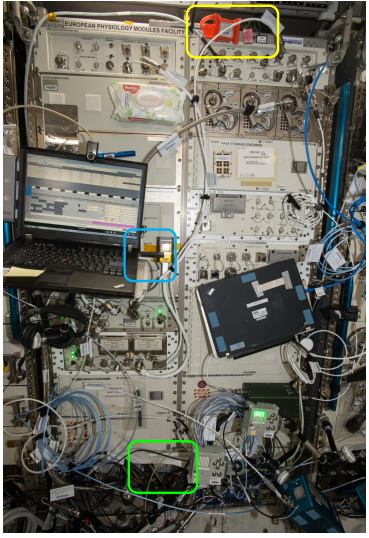

Figure 2: The Passive Detector Packages (PDP) from the DOSIS 3D project and the NASA RAM detectors (yellow); the NASA REM detector in the front of the EPM Rack (blue); the DOSIS-MAIN-BOX beneath the EPM rack (green) with three green status LEDs. (Image, caption courtesy T. Berger, DLR)

DOSTEL (DOSimetry TELescope)

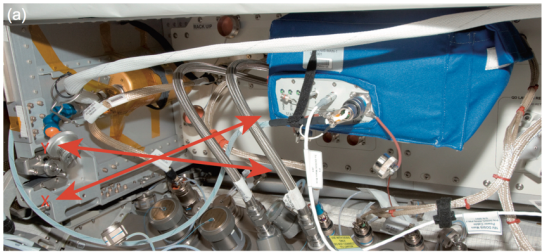

Figure 3: The DOSIS-MAIN-BOX (blue box) mounted beneath the EPM rack in Columbus. Shown is also the viewing direction of the DOSTEL-1 (X) and the DOSTEL-2 (Y) instruments. [1] (Source: NASA/ESA)

→ Each DOSTEL houses two passivated implanted planar silicon (PIPS) detectors (D-1 and D-2). [1]

- 315 μm thick, arranged 15 mm apart.
- Active area of 6.93 cm^2 .
- Opening angle: 120°.
- Geometry factor: 824 $mm^2 \cdot sr$.
- E_Δ range: 0.07 - 165 MeV.

REM (Radiation Environment Monitor)

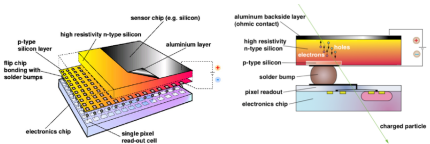

Figure 4: Medipix chip and Timepix assembly. (Source: CERN/Medipix.)

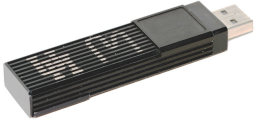

Figure 5: Radiation Environment Monitor.

- Hybrid silicon pixel detector utilizing Medipix/Timepix technology (CERN).
- 256×256 pixels, each with a 55μm pitch (1.982cm^2).
  - $\text{REM}^{1007}_{\text{D03}}$: 300 μm thick.
  - $\text{REM}^{5001}_{\text{J02}}$: 500 μm thick.
  - $E_{\Delta,pixel}$ range[1]: 5 - 800 keV.
- Opening angle: 4π.
- Nominally run in ToT (time over threshold) mode; acquisition time adjusted based on pixel occupancy and trending.

[1] 0.005 - 2 MeV per pixel with advanced calibration.

Analysis Overview

- All daily dosimetry data and energy loss spectra masked for:
  - days with less than 80ks of data;
  - days in which the dose in the SAA for REM varies by more than a factor of 1.4, for which we assume the SSC (and/or REM) was temporarily moved away from the nominal configuration.
- Raw frame data from REMs are collected on the SSCs, down-linked, and analyzed on the ground.
  - Trivial to analyze frame/cluster data to generate products that are similar to other instruments.
  - For this comparison, REM dosimetric and cluster observables integrated into 100-/20-s “bins” with start/stop times identical to DOSTEL’s.

Environment Definitions

For a more direct comparison, GCR/SAA are categorized differently.

Dosimetry:

- Magnetic field and L-shell
  - GCR: $|B| \geq 23\mu T$, $L \geq 3$
  - SAA: $|B| < 23\mu T$, $L < 3$
- Note: Magnetic field calculated with IGRF12.
  - Geomagnetic field model modulates in time.

Energy loss:

- GCR/SAA categorization is performed using DOSTEL's count rate threshold (30Hz) to switch between the so-called GCR mode and SAA modes.
- Specifically, the start and stop time of each mode is used to artificially "bin" $\mathrm{REM}^{5001}_{\mathrm{J02}}$ data.

GCR Definition with B/L

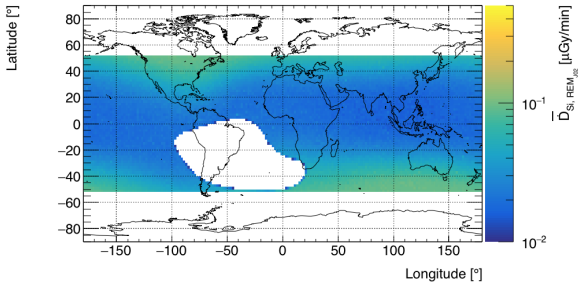

(a) $\bar{\dot{D}}_{Si,\mathrm{REM}^{5001}_{\mathrm{J02}}}$

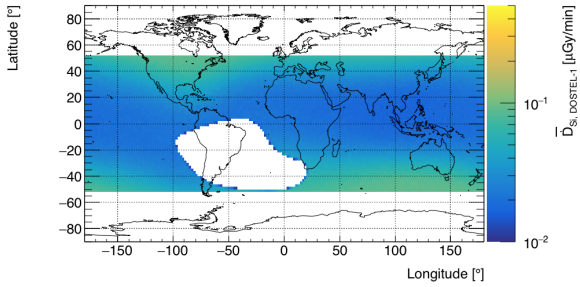

(b) $\bar{\dot{D}}_{Si,\mathrm{DOSTEL-1}}$

Figure 6: Average dose rate in the GCR region using data from [2013-11-10, 2016-02-09). GCR is defined as $|B| \geq 23\mu T$, $L \geq 3$.

SAA Definition with B/L

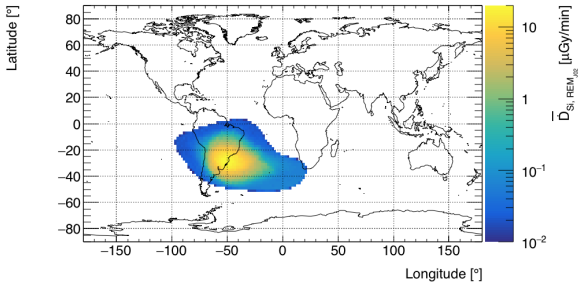

(a) $\bar{\dot{D}}_{Si,\mathrm{REM}^{5001}_{\mathrm{J02}}}$

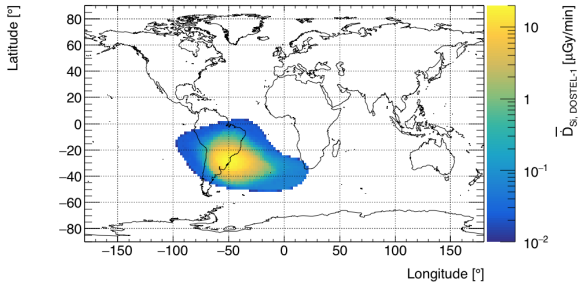

(b) $\bar{\dot{D}}_{Si,\mathrm{DOSTEL-1}}$

Figure 7: Average dose rate in the SAA region using data from [2013-11-10, 2016-02-09). The SAA is defined as |B|$< 23\mu$T, L< 3.

Total Combined Environment

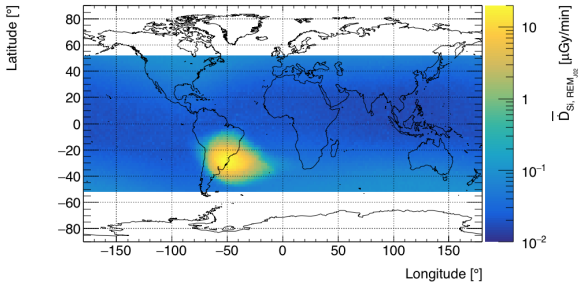

(a) $\bar{\dot{D}}_{Si,\mathrm{REM}^{5001}_{\mathrm{J02}}}$

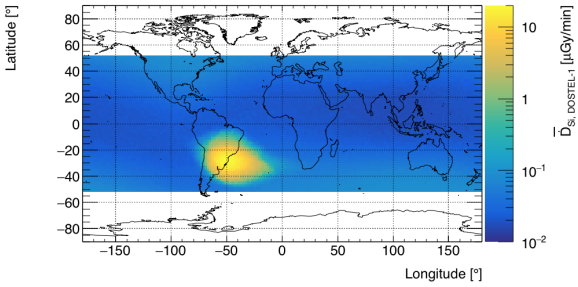

(b) $\bar{\dot{D}}_{Si,\mathrm{DOSTEL-1}}$

Figure 8: Average dose rate in LEO using data from [2013-11-10, 2016-02-09].

Rate Maps

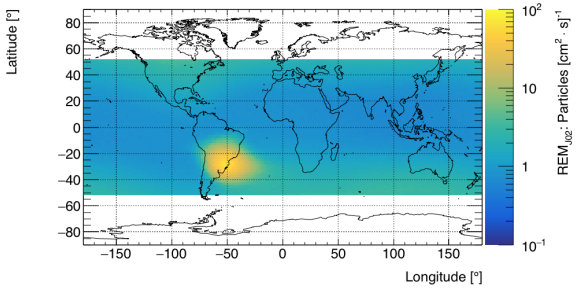

(a) $\mathrm{REM}_{\mathrm{J02}}^{5001}$

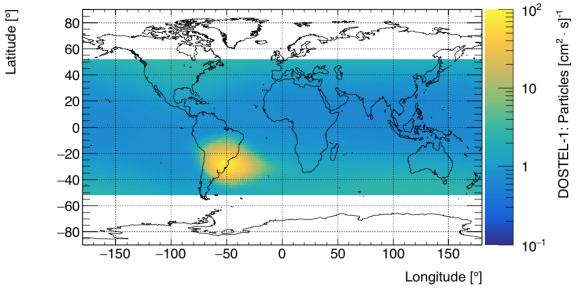

(b) DOSTEL-1

Figure 9: Event rates in DOSTEL-1 and $\mathrm{REM}_{\mathrm{J02}}^{5001}$ as a function of trajectory while co-located in Columbus for [2013-11-10, 2016-02-09).

An Example Day

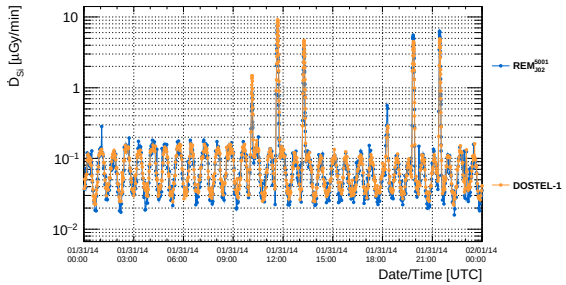

(a) Dose rate

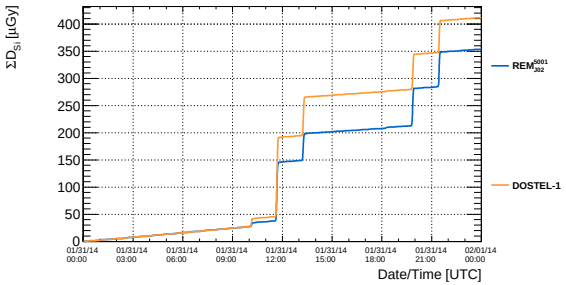

(b) Cumulative dose

Figure 10: Dose rate in silicon per interval in $\text{REM}^{5001}_{\text{J02}}$ and DOSTEL-1 covering [2014-01-31, 2014-02-01).

Daily Dose

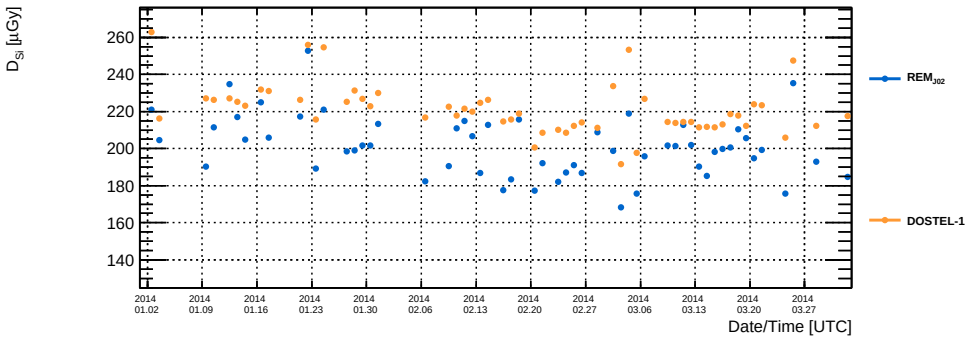

Figure 11: Daily dose in silicon for DOSTEL-1 and $\mathrm{REM}_{\mathrm{J02}}^{5001}$ for [2014-01-01, 2014-04-01).

Daily Dose in GCR/SAA

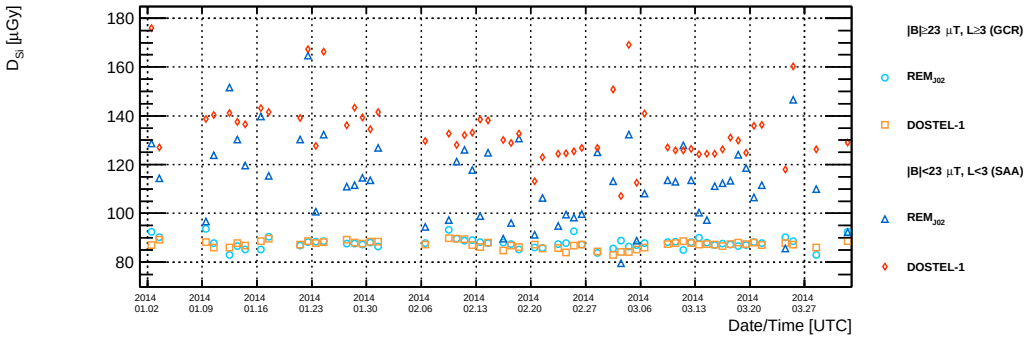

Figure 12: Daily dose in GCR ($|B| \geq 23\mu T$, $L \geq 3$) and the SAA ($|B| < 23\mu T$, $L < 3$) in silicon for DOSTEL-1 and $\text{REM}^{5001}_{\text{J02}}$ for [2014-01-01, 2014-04-01).

Daily Dose Ratios

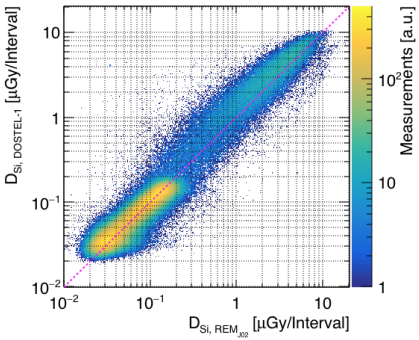

Figure 13: Dose rate in DOSTEL-1 versus $\mathrm{REM}_{\mathrm{J02}}^{5001}$ in time for each measurement in [2013-11-10, 2016-02-09).

- In GCR, $\mathrm{REM}_{\mathrm{J02}}^{5001}$ and DOSTEL-1 are very close to each other; quite some spread in the SAA though.
- Daily dose ratio for $\mathrm{REM}_{\mathrm{J02}}^{5001}$/DOSTEL-1:
  - GCR: $\mu = 1.01, \sigma = 0.02$
  - SAA: $\mu = 0.86, \sigma = 0.10$

Energy Loss

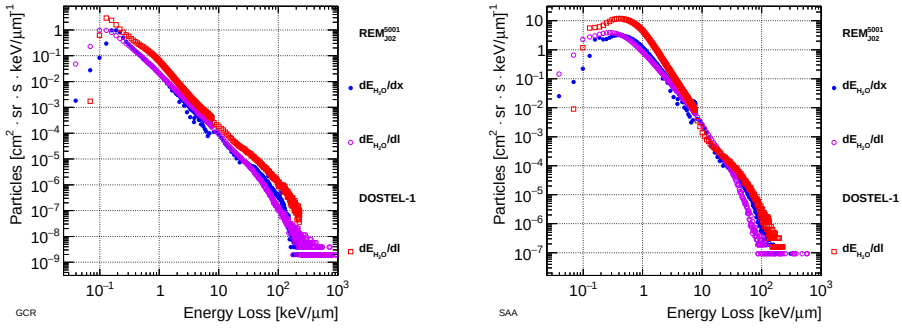

(a) GCR (b) SAA

Figure 14: Energy loss in water for DOSTEL-1 (DOSIS3D) and $\mathrm{REM}^{5001}_{\mathrm{J02}}$ for [2013-11-10, 2016-02-09). Note that DOSTEL-1's GCR/SAA modes and binning has been applied to $\mathrm{REM}^{5001}_{\mathrm{J02}}$ data. The differences in spectra are undergoing further analysis.

<Q>

Table 1: <Q> for DOSIS-3D, DOSTEL-1, and $\text{REM}_{\text{J02}}^{5001}$ in the GCR and SAA environments.

Detector	$<Q>_{\text{GCR}}$	$<Q>_{\text{SAA}}$	Energy Loss Type	Notes
DOSIS-3D	3.13	1.20	$dE_{\Delta,H_2O}/dl$	[1]
$\text{REM}_{\text{J02}}^{5001}$	2.49	1.32	$dE_{\Delta,H_2O}/dx$	
	1.93	1.22	$dE_{\Delta,H_2O}/dl$	

Observations

Trending in the GCR environment (identified with |B|/L) is incredibly stable in DOSTEL-1 and $\text{REM}^{5001}_{\text{J02}}$.

- → The agreement for daily dose in GCR is stellar, within 2%.
- → Fluctuations in the daily dose in trapped/SAA are within $14 \pm 10\%$, considerably small given the fact that these detectors are not truly co-located.

The differences in the energy loss spectra are substantially larger than those observed in dosimetry and are currently under analysis.

- → $\sim 5\times$ higher in DOSTEL-1 than $\text{REM}^{5001}_{\text{J02}}$ for GCR; $\sim 6\times$ in the SAA.
- → Comparisons between IV-TEPC/$\text{REM}^{5001}_{\text{J02}}$ and RAD/$\text{REM}^{1007}_{\text{D03}}$ (c.f C. Zeitlin's talk) show differences that are on the order of a few percent.

RAD & REM

Detector Locations

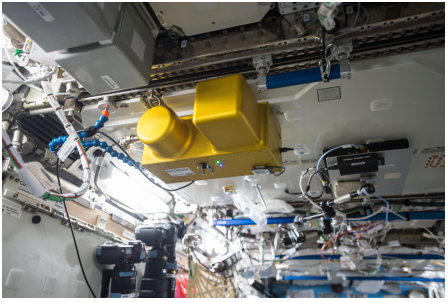

Figure 15: RAD at LAB1 O3.

Figure 16: $\text{REM}^{1007}_{\text{D03}}$, in the orange box, on SSC9.

ISS-RAD (Radiation Assessment Detector)

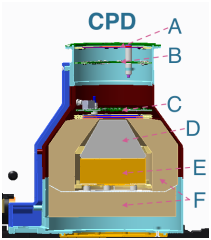

→ Here, we will only focus on the CPD in ISS-RAD (legacy design from MSL-RAD), specifically the B sub-detector.

- E_{Δ} range: 0.06 - 500 MeV.

Figure 17: Charged Particle Detector (CPD).

Detector	Material	Type	Purpose
A, B[2], C	Si, 300 μm	Solid State Detector	Charged particle spectroscopy.
D	BGO[3]	Scintillating calorimeter	Energy resolving detector.
E[2]	EJ260XL	Plastic Scintillator	High-energy particle + n^0 measurements.
F			Anti-coincidence

[2]Provides charged particle dosimetry.

[3]Bismuth Germanium Oxide.

Environment Definitions

For the RAD/REM dosimetry comparison, we only look at the first 10 months of RAD's deployment in the US Lab; GCR/SAA categorization is performed using geomagnetic field intensity and McIlwain L-Shell.

- → GCR: $|B| \geq 23\mu T$, $L \geq 3$
- → SAA: $|B| < 23\mu T$, $L < 3$

Comments:

- → |B| and L are calculated for every second of ISS trajectory and mapped back to instrument data during data processing.
  - ◎ Takes ∼1s to calculate a single trajectory point, i.e., latitude, longitude, altitude, B, and L; this is brute-force parallelized and run daily on a cluster through cron.

Analysis Overview

- For $\mathrm{REM}_{\mathrm{D03}}^{1007}$, raw frame/cluster data analyzed for the world maps; dose is integrated over all frames in a minute (normalized to the total acquisition time) and then integrated in each environment per day.
- All daily dosimetry data masked for days with less than 95% live time.

Dosimetry Maps

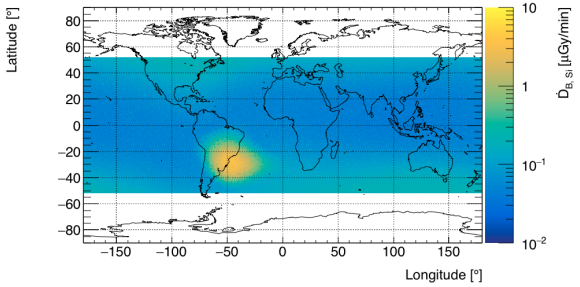

(a) RAD

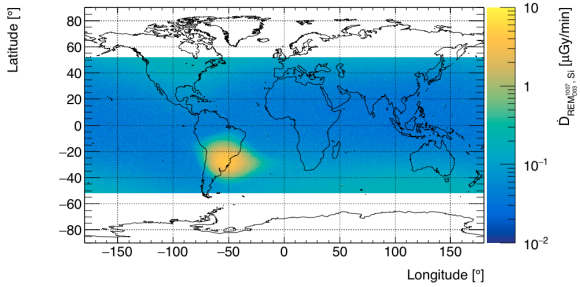

(b) REM

Figure 18: Dose rate in silicon for $\mathrm{RAD_B}$ and $\mathrm{REM}^{1007}_{\mathrm{D03}}$ as function of trajectory while co-located in the US Lab for [2016-02-01, 2017-01-01).

Rate Maps

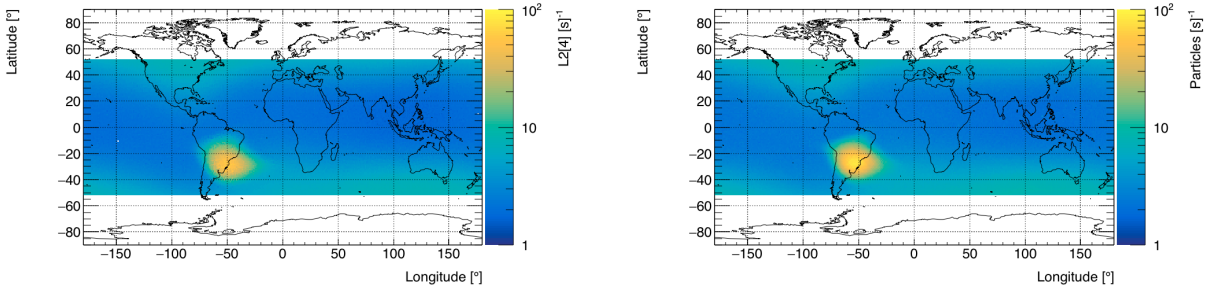

(a) RAD

(b) REM

Figure 19: Event rates in $\mathrm{RAD_B}$ and $\mathrm{REM}^{1007}_{\mathrm{D03}}$ as function of trajectory while co-located in the US Lab for [2016-02-01, 2017-01-01).

Daily Dosimetry: GCR/SAA

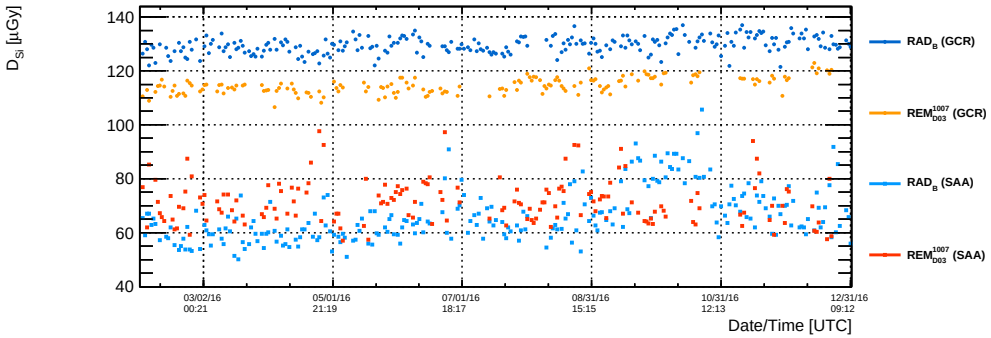

Figure 20: Daily dose for GCR and trapped/SAA in silicon for $\mathrm{RAD_B}$ and $\mathrm{REM^{1007}_{D03}}$ while co-located in the US Lab for [2016-02-01, 2017-01-01). Only days for which there is more than 95% live time are shown.

Dosimetry Comparisons

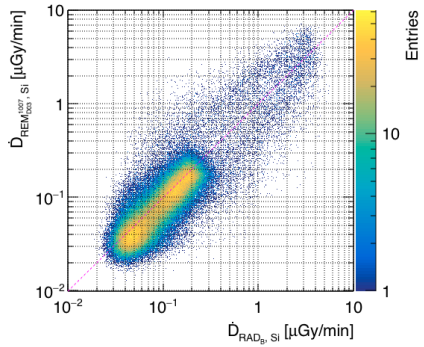

Figure 21: Dose rate in $\mathrm{REM}^{1007}_{\mathrm{D03}}$ versus $\mathrm{RAD_B}$ in time.

- $\mathrm{RAD_B}$ normally $\{^{\text{higher}}_{\text{lower}}\}$ than $\mathrm{REM}^{1007}_{\mathrm{D03}}$ at $\{^{\text{low}}_{\text{high}}\}$ doses $\{^{\text{GCR}}_{\text{SAA}}\}$.
  - Clearly seen in the daily dose.
- Daily dose ratio for $\mathrm{RAD_B}/\mathrm{REM}^{1007}_{\mathrm{D03}}$:
  - GCR: $\mu = 1.13, \sigma = 0.03$
  - SAA: $\mu = 0.92, \sigma = 0.15$

Observations

The trending observed in $\mathrm{RAD_B}$ and $\mathrm{REM}^{1007}_{\mathrm{D03}}$ is characteristic of shielding differences. $\mathrm{REM}^{1007}_{\mathrm{D03}}$ is mounted to a SSC and appears to be situated in a place which is less shielded than LAB1 03.

- → Thinner shielding results in lower GCR dose rates and higher trapped/SAA dose rates; very thin locations result in substantially higher dose rates through the trapped/SAA environment.
- → Thicker shielding generates more secondaries in GCR and produces higher dose rates (relative to a less shielded area) while also bringing the trapped/SAA dose rates down.
  - ◎ Trapped/SAA dose rates decrease faster than the increase in GCR dose rates.

Summary

Remarks

In looking over multiple years of data from significantly different silicon-based detectors, we see pretty good agreement in the dosimetry; more analysis and interpretations needed on the energy loss spectra.

- Several years of dosimetric comparisons between DOSTEL-1 and $\text{REM}^{5001}_{\text{J02}}$ show that daily doses are on average within:
  - $\sim$2% for GCR; $\sim$14% for the trapped/SAA environment.
- Similarly, for $\sim$10 months of RAD_{B} and $\text{REM}^{1007}_{\text{D03}}$ data:
  - On average within $\sim$13% for GCR; $\sim$8% for the trapped/SAA environment.
- Localized shielding drive most of the disagreement between the daily doses.
  - Temporary SSC/REM relocations also a nuisance parameter.

Acknowledgements

Thanks to:

- → T. Berger, D. Matthiä, & S. Burmeister for discussions and data from DOSTEL/DOSIS-3D.
- → N. Stoffle for discussions and images on the ISS CAD models and REM.
- → C. Zeitlin for discussions on RAD.
- → X. Xu & M. Clowdsley for generating/providing the GCR/SAA flags utilizing AP8/AP9.

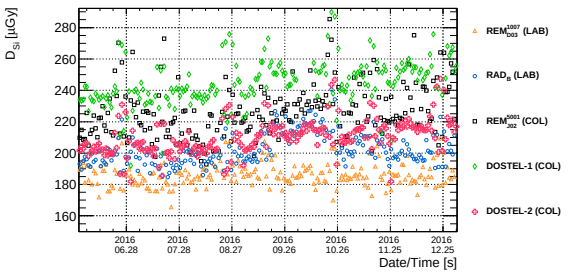

Figure 22: Daily dose in silicon for DOSTEL-1, DOSTEL-2, $\mathrm{RAD_B}$, $\mathrm{REM}^{1007}_{\mathrm{D03}}$, & $\mathrm{REM}^{5001}_{\mathrm{J02}}$.

References


T. Berger, S. Burmeister, D. Matthiä, et al.
»DOSIS & DOSIS 3D: radiation measurements with the DOSTEL instruments onboard the Columbus Laboratory of the ISS in the years 2009–2016«
J. Space Weather Space Clim., 2017, vol. 7, p. A8

Additional Material

Instrument Specific

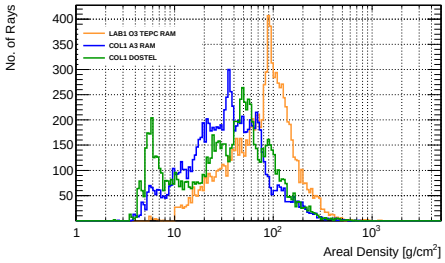

(a) Shielding distribution

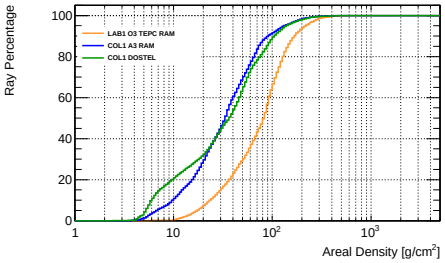

(b) Cumulative shielding distribution

Figure 23: Shielding distributions for the US Lab where the TEPC, RAM, & RAD detectors are nominally installed and locations in Columbus where the RAM and DOSTEL detectors are installed. (Images, courtesy of N. Stoffle)

Shielding Map

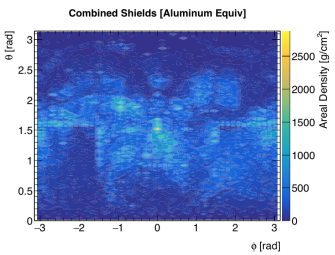

(a) TEPC, RAM, & RAD in US LAB1 O3, ρ_A=93.7g/cm^2 (Al-eq.)

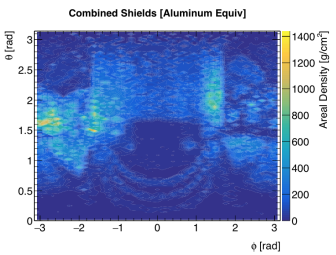

(b) DOSTEL in COL1, ρ_A=50.1g/cm^2 (Al-eq.)

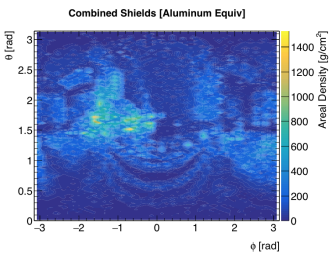

(c) RAM in COL1 A3, ρ_A=47.0g/cm^2 (Al-eq.)

Figure 24: Shielding distributions around different detectors in the US Lab and Columbus. (Images, courtesy of N. Stoffle)

ISS Orientation

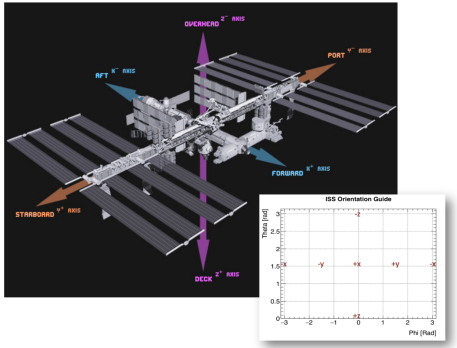

Figure 25: ISS orientation and coordinate system. (Image, courtesy of N. Stoffle)

Instrument Specific

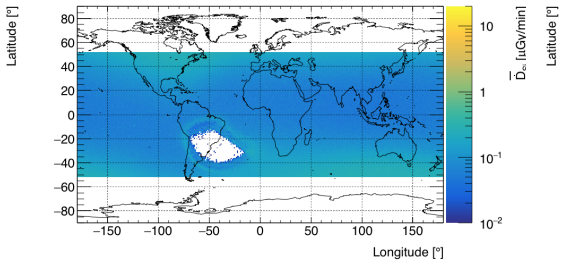

(a) GCR

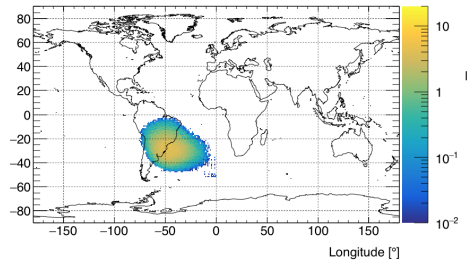

(b) SAA

Figure 26: Average daily dose rate in silicon in RAD with instrument-specific GCR/SAA separation.

B/L

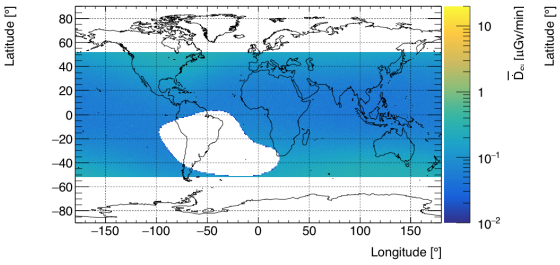

(a) GCR

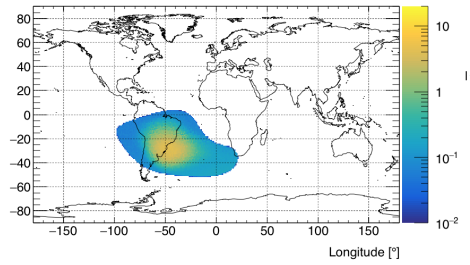

(b) SAA

Figure 27: Average daily dose rate in silicon in RAD with GCR/SAA separation based on magnetic field intensity and L-shell.

AP8×geoffb

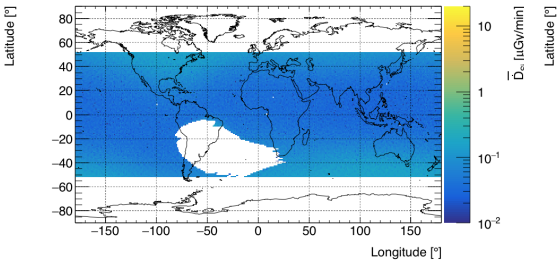

(a) GCR

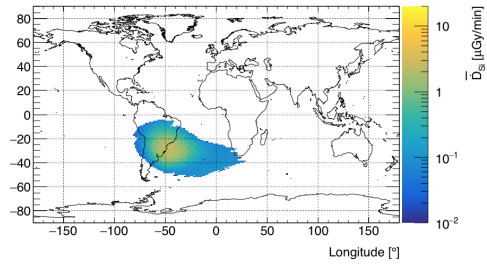

(b) SAA

Figure 28: Average daily dose rate in silicon in RAD with GCR/SAA separation based on based on proton flux contributions in a given location using AP8×geoffb.

AP9

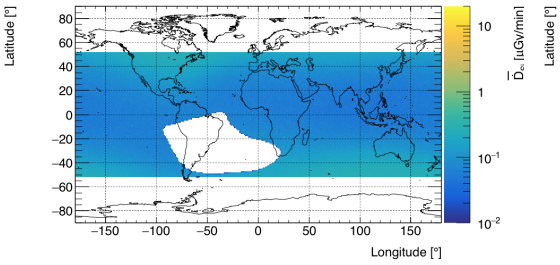

(a) GCR

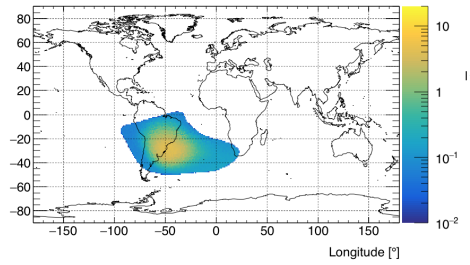

(b) SAA

Figure 29: Average daily dose rate in silicon in RAD with GCR/SAA separation based on proton flux contributions in a given location using AP9.

Magnetic Field & L-Shell

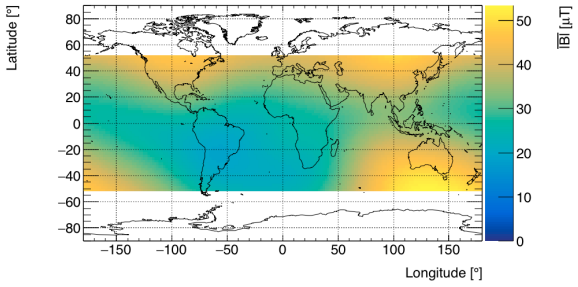

(a) |B|

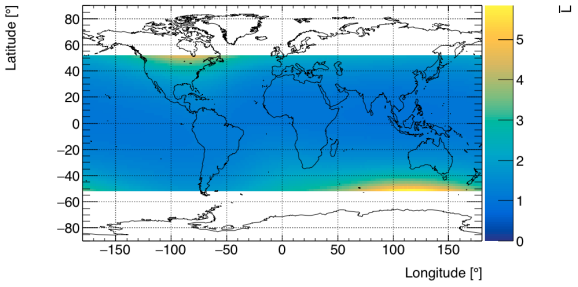

(b) L-shell

Figure 30: Average magnetic field intensity (|B|) and Mc-Ilwain L-shell as a function of orbital trajectory for [2013-11-10, 2016-02-09).

|B| & L Maps

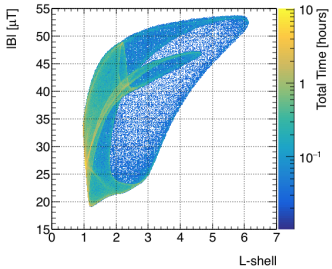

(a) Total acquisition time.

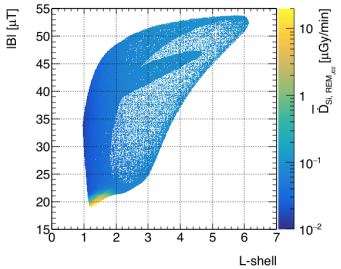

(b) $\text{REM}^{5001}_{\text{J02}}$

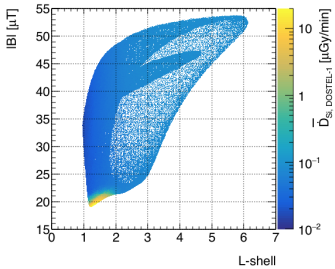

(c) DOSTEL-1

Figure 31: Total acquisition time and average dose rates for $\text{REM}^{5001}_{\text{J02}}$ and DOSTEL-1 as a function of geomagnetic field intensity and L-shell for [2013-11-10, 2016-02-09).

$\dot{D}_{Si}$ Comparison

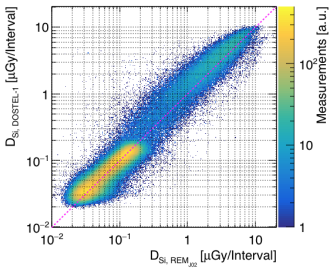

(a) Combined environment.

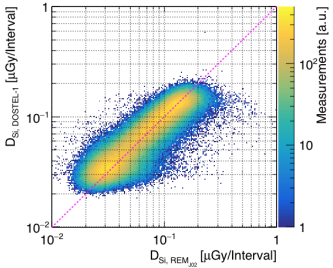

(b) GCR

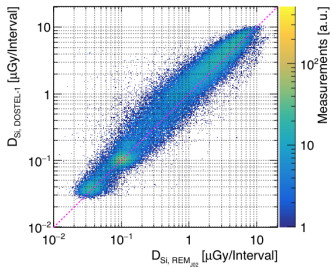

(c) SAA

Figure 32: Dose rate in DOSTEL-1 versus $\text{REM}_{\text{J02}}^{5001}$ in time for each measurement in [2013-11-10, 2016-02-09); GCR and SAA are defined using the |B| & L definitions on page 10.

Daily Dose Ratios: DOSTEL/REM

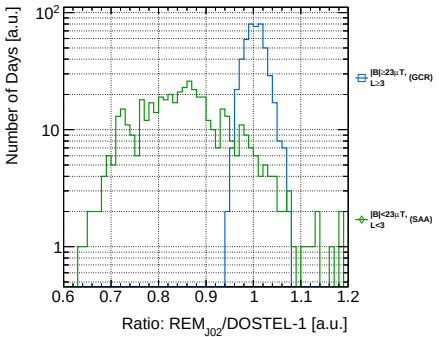

Figure 33: Ratio of daily dose in $\mathrm{REM}_{\mathrm{J02}}^{5001}$ to DOSTEL -1 in GCR and trapped/SAA for [2013-11-10, 2016-02-09).

Daily Dose from GCR

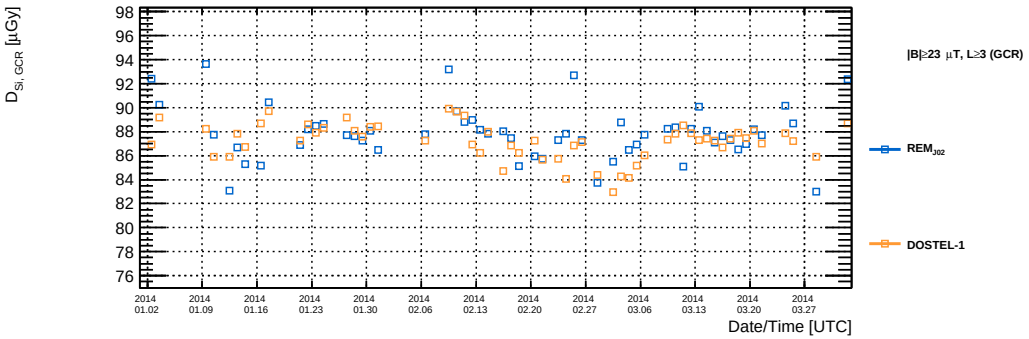

Figure 34: Daily dose from GCR ($|B| \geq 23\mu T$, $L \geq 3$) in silicon for [2014-01-01, 2014-04-01).

Daily Dose in the SAA

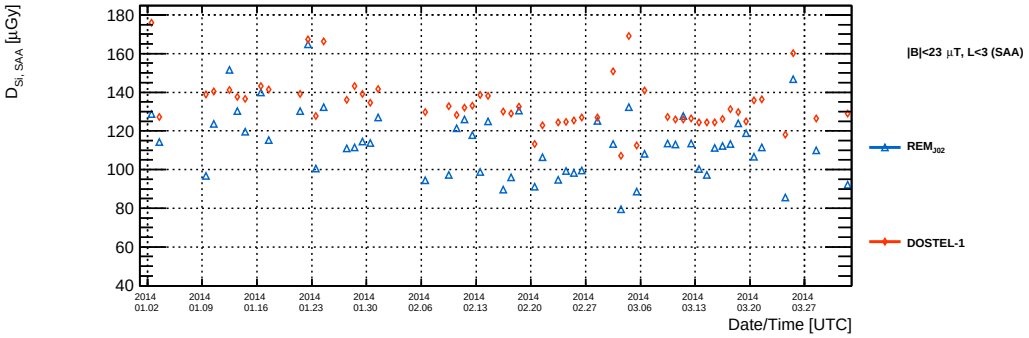

Figure 35: Daily dose in the SAA ($|B| < 23\mu T$, $L < 3$) in silicon for [2014-01-01, 2014-04-01).

Chord Length Approximation

In pixelated detectors, such as Timepix, we calculate the projected track through the detector assuming that each particle fully penetrates.

→ Also have the ability to use the average chord length (or average path length).

The average chord length for an isotropic environment is simply:

$$4 \times \frac{Volume}{Surface\ Area}$$

For most planar detectors, this reduces to $2h$, where h is the thickness of the active detector. Since the Timepix detectors can readout any incoming particle at all incident angles, we use the full solution, which includes each side.

→ For $\text{REM}^{5001}_{\text{J02}}$, whose thickness is 500µm, the average chord length is 933µm.
- Timepixes with a thickness of 300µm will have an average chord length of 575µm.

REM: dE/dx v. dE/dl

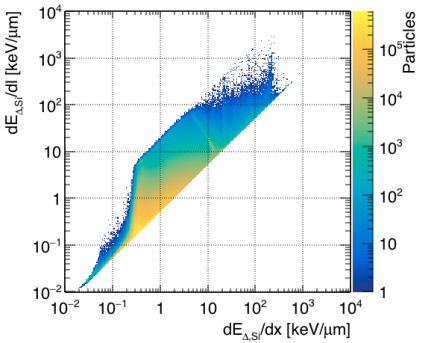

Figure 36: Comparison of dE/dx v. dE/dl in $\text{REM}^{5001}_{\text{J02}}$ for the total combined LEO environment. Note that tracks require at least 4 pixels.